

## **COST OPTIMISATION OF MOORING SYSTEMS FOR OFFSHORE FLOATING PLATFORMS IN DEEP WATER**

**<sup>1</sup>Ovie A. Ophori, <sup>2\*</sup>Tobinson. A. Briggs, <sup>3</sup>Endurance. O. Diemuodeke**

*<sup>1</sup>Offshore Technology Institute, The University of Port Harcourt*

*<sup>2,3</sup>Mechanical Engineering, University of Port Harcourt*

*\*Email: tobinson.briggs@uniport.edu.ng*

---

**ABSTRACT:** *There is a need to minimize the cost of mooring systems, which can take up a large number of investments in offshore operations as human activities move into deeper waters. A methodology for cost optimisation of the mooring system of floating structures in deep water is presented. A techno-economic model was developed based on the quasi-static taut leg multi-component equations and simple cost relations in Engineering Equation Solver (EES), used with MS Excel for the analysis. Manufacturing and pre-installation costs were combined as the cost driver. Two mooring line configurations, chain-wire-chain and chain-polyester-chain were analysed, and the genetic algorithm incorporated in EES was used to obtain optimal costs. The results showed that depending on the pre-installation cost; optimal cost resulted from a trade-off between sizes of components and number of lines. It was also revealed that components of multi-component lines should have Minimum Breaking Strength (MBS) as close as possible to eliminate cost wastage. The chain-polyester-chain (C-P-C) system, for the selected water depth of 1473m and angle at TDP of 25<sup>0</sup> for a load of 44MN, produced a 35% cost reduction over the chain-wire-chain (C-W-C) system.*

**KEYWORDS:** cost optimisation, mooring system, floating structure, techno-economic model

---

### **INTRODUCTION**

Operations by man are increasingly moving into deeper water. Since deepwater exploration began in the 1970s (Zhang et al., 2019), exploration and production in deepwater, greater than 500 [m], has expanded dramatically during the past decade, to the point where it has become a significant component of the petroleum industry's annual upstream budget (Pettingill and Weimer, 2002). The existing deepwater oil fields in the world are mostly distributed in Atlantic deepwater basins of Brazil, the Gulf of Mexico and West Africa deepwater areas and the existing deepwater gas fields are distributed in East Africa, the Barents Sea, Northwest shelf of Australia, Eastern Mediterranean, and other deepwater areas (Zhang et al., 2019). Deepwater exploration and production are expected to increase as onshore and shallow offshore production declines, to meet growing global oil and gas demands.

Globally, majority of the biggest deepwater oilfields are located in offshore Brazil, such as Libra, Lula and Franco, and the Gulf of Mexico in the USA, such as Julia and

Mad dog, in depths of water ranging from 1300m to 2200m (Zhang et al.). Also, many of the sizeable deepwater gas fields discovered, in depths of water greater than 500 [m], are located offshore Mozambique, Australia, and Israel in water depths ranging from 500m to 1700m, and a large gas field in Senegal in a water depth of 2700m. In offshore West Africa, Gulf of Guinea, large fields are distributed in Angola, Senegal, Nigeria and Ghana.

Notable oil and gas fields that have been discovered in offshore Nigeria are listed in Table 1. Due to challenges posed by deeper water, floating platforms are the only practicable structures for exploring and producing oil and gas in deep water. An essential part of the exploration and production of oil and gas offshore is station-keeping of platforms. The platform has to remain within a specified radius of operation on the water surface for continuation and completion of the work process and safety and environmental reasons. The mooring system is an essential part of station-keeping, especially for floating production platforms. As new frontiers in the industry are explored, including ultra-deepwater, and arctic areas. The operations adjacent to other installations become more frequent and floating offshore platforms become more extensive; the requirements for mooring systems increase in complexity for mobile and permanent floating platforms.

**Table 1 Notable oil and gas fields in Nigeria**

Field	Water depth (m)	Operator	Reserve
Agbami	1463	Chevron	Estimated total reserves: $136 \times 10^6$ tons
Akpo	1100 – 1700	Total	Proven and potential reserves: $85 \times 10^6$ tons condensate oil and $28.3 \times 10^9$ m <sup>3</sup> natural gas
Bonga	>1000	Shell	Recoverable reserves: $82 \times 10^6$ tons
Egina	1750	Total	Probable reserves: $75 \times 10^6$ tons
Erha	1000 – 1200	ExxonMobil	Recoverable reserves: $68 \times 10^6$ tons
Usan	750 – 850	ExxonMobil	Recoverable reserves: $68 \times 10^6$ tons

Source: Zhang et al., 2019

Increasing water depth poses increasing difficulties in the design and implementation of mooring systems. Increasing water depth also increases the cost of the mooring system significantly. There exists a need to find cost solutions of best value without compromising the safety of operations and ensuring that compliance with government regulations, local and international standards are met.

This work aims to optimise the cost of mooring systems of offshore floating platforms in deep water by carrying out a techno-economic analysis of the mooring lines of the system. The objectives include;

- i. Data gathering.
- ii. Modelling of the mooring system.
- iii. Performance of techno-economic analysis.
- iv. Performance of Cost optimisation using a genetic algorithm.

This study attempted to propose optimal cost solutions of mooring systems of offshore floating platforms in deep water from a technical and economic perspective. This work is intended to aid design, planning and implementation of mooring systems for effective station keeping of floating platforms and thus safe and reliable production of oil and gas from deepwater developments. Particular focus will be on the Nigerian offshore environment and offshore West Africa (Gulf of Guinea).

This work only covers the techno-economic analysis of the mooring lines, as a sub-system of the mooring system of a permanent floating structure, and was modelled accordingly. The application and suitability of market available mooring line materials; chain, steel wire rope and polyester (synthetic fibre), were studied and optimisation was conducted based on the sizes and properties of these mooring line materials. The techno-economic performance of multi-component lines; chain-wire-chain and chain-polyester-chain were compared. However, detailed individual study and designs of the mooring lines were not done in this work. Also, anchor, connector and on-vessel equipment selection were not considered in this work.

## **METHODOLOGY**

### **System description**

The mooring line catenary configuration is the fundamental element of mooring analysis. The catenary configuration is a good representation of the static shape of a mooring line hanging under its self-weight, that is, from fair-lead to touch down point (TDP) on the seabed. Figure 1 shows a simple 2D geometry of the catenary configuration, with three sections – 1, 2 and 3. A structure floating on the sea surface is moored to the seafloor utilizing multi-component lines, with a single line represented in Figure 1.

The mooring section one, indicated as (1) in Figure 1, has a chain component – referred to as bottom chain – and it is attached to the anchor at touch down point (TDP). A chain mooring component is used in this section because of its higher resistance to abrasion by the seabed. The mooring section two, indicated as (2) in Figure 1, has a steel wire rope or polyester (synthetic fibre) component. Steel wire ropes and polyester are much lighter and more economical to use in deep water. They also provide minimum offset required in deep water due to having less of a catenary effect. Section two makes up a large majority of the length, depth and horizontal distance of the line. The mooring section three, indicated as (3) in Figure 1, has a chain component, referred to as the top chain. A relatively shorter chain is used here and held in place on the structure utilizing a chain stopper. A chain is better held in place than wire rope or polyester for permanent floating structures. The TDP is taken as a point of reference and its assigned a local position of [0,0]. The angle,  $\theta$ , is the angle of the line to the horizontal, seafloor, at touch down point.

The horizontal distance, from TDP to the vessel, is represented by the letter,  $x$ , and the vertical distance or depth, from the seafloor to sea surface, is represented by the letter,  $h$ . The horizontal distance of each component is represented by,  $x_i$ , and the vertical distance is represented by,  $h_i$ , where,  $i = 1,2,3$ ; is the section number of a component in the studied line.

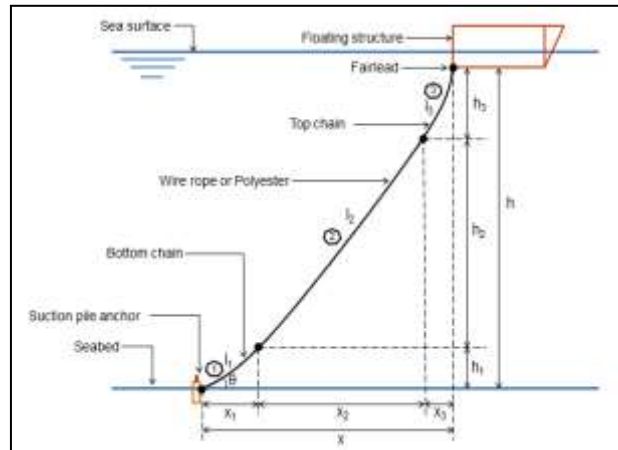


**Figure 1: Geometry of a 2D multi-component taut mooring configuration**

### Governing equations

The mooring lines exert restraining tension forces on the floating structure due to their weight and elastic properties. The tensions on the lines are calculated from the catenary equations. In a condition of static equilibrium of a segment, the mooring line axial tension can be predicted by the equations:

For a catenary mooring line of a single component, the tension,  $T(N)$ , on the line can be represented by (Ma et al., 2019):

$$\frac{dT}{dl} - w \sin \theta = 0 \quad (1)$$

$$\frac{d\theta}{dl} - \frac{w \cos \theta}{T} = 0 \quad (2)$$

Imposing boundary conditions at fairlead and the seafloor, the solutions of the equations become;

$$l(x) = \frac{T_H}{w} \sinh \left( \frac{w}{T_H} x \right) \quad (3)$$

$$h(x) = \frac{T_H}{w} \cosh \left( \frac{w}{T_H} x \right) - \frac{T_H}{w} \quad (4)$$

where  $l(x)$  (m) is the length of the line from TDP,  $x$  (m) is the horizontal distance from TDP towards the vessel, or floating structure,  $T_H$  (N) is mean horizontal environmental load,  $w$  (N/m) is the wet weight of the line,  $h$  (m) in height from the seabed.

Equations (3) and (4) can be used to plot the mooring line profile. Equation (5) can also be used to estimate the length of the line from TDP and the tension along the segment of the line is represented by Equation (6).

$$l = h \sqrt{\left(h + 2 \frac{T_H}{w}\right)} \quad (5)$$

$$T(l) = T_H + wh \quad (6)$$

If the maximum tension on a line ( $T_{max}$ ) is known, the minimum length of the line ( $l_{min}$ ) can be computed from equation (6).

$$l_{min} = h \sqrt{\left(2 \frac{T_{max}}{w} - 1\right)} \quad (7)$$

The total horizontal length,  $X$  (m), from anchor point to floating structure is computed from equations (7) and (8), where  $l_s$  (m) is suspended length of line.

$$X = l - l_s + x \quad (8)$$

$$X = l - h \sqrt{\left(2 \frac{T_{max}}{w} - 1\right)} + x \quad (9)$$

For multi-component mooring lines, represented in Figure 1, the equations become more complex as the formulations for each component depend on parameters from preceding components. The equations for multi-component moorings are represented by Equations (9) through (15) as, thus, (Xue et al., 2018):

$$x_1 = \frac{T_H}{w_1} \left[ \sinh^{-1} \left( \frac{w_1 l_1}{T_H} + \tan \theta_1 \right) - \sinh^{-1}(\tan \theta) \right] \quad (10)$$

$$h_1 = \frac{T_H}{w_1} \left[ \cosh \left( \frac{w_1 x_1}{T_H} + \sinh^{-1}(\tan \theta) \right) - \cosh(\sinh^{-1}(\tan \theta)) \right] \quad (11)$$

$$x_2 = \frac{T_H}{w_2} \left[ \sinh^{-1} \left( \frac{w_1 l_1 + w_2 l_2}{T_H} + \tan \theta \right) - \sinh^{-1} \left( \frac{w_1 l_1}{T_H} + \tan \theta \right) \right] \quad (12)$$

$$h_2 = \frac{T_H}{w_2} \left[ \cosh \left( \frac{w_2 x_2}{T_H} + \sinh^{-1} \left( \frac{w_1 l_1}{T_H} + \tan \theta \right) \right) - \cosh \left( \sinh^{-1} \left( \frac{w_1 l_1}{T_H} + \tan \theta \right) \right) \right] \quad (13)$$

$$x_3 = \frac{T_H}{w_3} \left[ \sinh^{-1} \left( \frac{w_1 l_1 + w_2 l_2 + w_3 l_3}{T_H} + \tan \theta \right) - \sinh^{-1} \left( \frac{w_1 l_1}{T_H} + \tan \theta \right) \right] \quad (14)$$

$$h_3 = \frac{T_H}{w_3} \left[ \cosh \left( \frac{w_3 x_3}{T_H} + \sinh^{-1} \left( \frac{w_1 l_1 + w_2 l_2}{T_H} + \tan \theta \right) \right) \dots \right. \\ \left. \dots - \cosh \left( \sinh^{-1} \left( \frac{w_1 l_1 + w_2 l_2}{T_H} + \tan \theta \right) \right) \right] \quad (15)$$

Equations (1) through (15) are quasi-static solutions, damping, fluid acceleration and added mass are ignored. The dynamic representation of a mooring line accounting for added mass and damping is given by Equation (16) (Xue et al., 2018):

$$M_a \frac{d^2x}{dt^2} + C \frac{dx}{dt} + K_s x = F_{static} + F_{WF} + T_W \quad (16)$$

Where  $x$  is the displacement vector from mean position,  $M_a$  (kg),  $C$  (Ns/m), and  $K_s$  (N/m) are matrices of mass, damping, stiffness, respectively:  $F_{static}$  (N) is the static load,  $F_{WF}$  (N) is the first-order wave loads which are imposed at wave frequency and  $T_W$  (N) is the tension from the mooring system; it is taken as the summation of the pretension. The mooring line tension induced by the first-order wave loads. However, the quasi-static equations are only considered in this work as a first approximation of the understanding of multi-component mooring system.

The cost of manufacturing or procurement of the mooring lines and pre-installation costs are considered in the cost analysis. The equations are simplified and are represented by:

$$C_{man} = n_{ml} \times \sum C_{Ni} W_i l_i \quad (17)$$

$$C_{ins} = C_{iv} \times \left( \frac{n_{ml}}{I_r} \right) \quad (18)$$

where,  $C_{man}$  (\$) is the cost of manufacturing of the mooring lines,  $C_{ins}$  (\$) cost of pre-installation of lines,  $n_{ml}$  (-) is the number of mooring lines,  $C_{Ni}$  (\$/N) is the cost per unit dry weight of mooring line component,  $C_{iv}$  (\$/day) and  $I_r$  (Line/day) are costs of installation of the vessel, and associated vessel personnel and mooring lines installation rate respectively.

This work aims to minimize the total cost of manufacturing and pre-installation. The objective function is given as;

$$MIN = C_{man} + C_{ins} \quad (19)$$

The constraint is the maximum tension on one line must be lesser than the minimum of the maximum tension allowable for a single component in the line. This is expressed as;

$$T < 0.6 \times \text{minimum MBL} \quad (20)$$

for intact lines, and

$$T < 0.8 \times \text{minimum MBL} \quad (21)$$

in situations of line failures.  $T$  (N) is tension on one line, and  $MBL$  (N) is minimum breaking load of a component, chain, wire rope or polyester. Tension on one line is expressed as;

$$T = \sqrt{T_H^2 + T_V^2} \quad (22)$$

and

$$T_H = T_p + \frac{W}{n_{mt}} \quad (23)$$

$$T_V = \sum w_i l_i \quad (24)$$

where  $T_V$ (N) is vertical tension,  $T_p$ (N) is the pretension of line,  $W$  (N) is external load from the environment. Pre-tension of the line is 10 – 20% of minimum MBL.

This work considered a studless chain, grade R4, therefore, its wet weights and minimum breaking strength can be related, respectively, as (Ma et al., 2019):

$$w = 0.171 \times d_c^2 \quad (25)$$

$$MBL = 0.274 \times d_c^2 (44 - 0.08d_c) \quad (26)$$

whereas for rope, the wet weights and minimum breaking strength can be related, respectively, as (Ma et al., 2019):

$$w = 0.043 \times d_w^2 \quad (27)$$

$$MBL = 0.9 \times d_w^2 \quad (28)$$

and for polyester, the wet weights and minimum breaking strength can be related, respectively, as (Ma et al., 2019):

$$w = 0.0017 \times d_p^2 \quad (29)$$

$$MBL = 0.25 \times d_p^2 \quad (30)$$

### Assumptions

For simplicity and ease of computations, the assumptions made, without necessarily sacrificing accuracy, in the modelling and computations are:

- Mooring components are inelastic.
- Seabed surface is even.
- Added mass, fluid acceleration and damping are negligible.
- The load is mean horizontal environmental force from current, waves and wind.
- Pre-installation cost and installation rate of polyester and wire rope are similar.

### Optimisation in EES with genetic algorithm

The genetic algorithm implemented in EES is derived from the Pikaia optimisation program developed by Paul Charbonneau and Barry Knapp at National Center for Atmospheric Research (NCAR), United States of America. As described by the High Altitude Observatory (HAO) of the University Corporation for Atmospheric Research (UCAR), Pikaia is fully self-contained, optimisation subroutine for general purpose. It incorporates uniform one-point crossover or breeding, and uniform one-point mutation. Pikaia utilizes encoding based on a decimal alphabet of ten (10) integers (0 through 9), and the operations are carried out through platform-dependent functions, in FORTRAN.

HAO also states that the genetic algorithm differs from the Monte Carlo algorithm in two ways. The production of trial solutions from existing solutions happen through breeding and probability of selection of a solution to partake in a breeding event is proportional to the solution's fitness, implying that better solutions breed more frequently.

A description, by Mathworks, of a run-through of the working of the algorithm, is given thus:

- a) Creation of an initial random population
- b) Creation of sequences of newer populations. Individuals in the current generation are used in creating subsequent populations. To create newer populations, the following steps are performed:
  - i. Members of the current population are scored by computation of their fitness values. The values are referred to as raw fitness scores.
  - ii. The fitness scores are scaled and converted into more usable values range. The values are indicated as expectation values.
  - iii. Members, known as parents, are selected due to their expectation.
  - iv. Some individuals in the current population with lower fitness are picked as elite. The elite individuals pass to a subsequent population.
  - v. Children from parents are produced. The algorithm produces children by random changes made to a parent, termed mutation, or a combination of vector entries of parent pairs, termed crossover.
  - vi. The current population is replaced with children for the formation of a subsequent generation.
- c) The algorithm is stopped when a stopping criterion is satisfied, which could be the number of generations, time limit or fitness limit etc.

As the generations number increase, individuals in population converges to a minimum point. The algorithm is a flow chart format is shown in Figure 2.

### Input data

The input data in Table 1 was sourced from materials of a recent deepwater project in Nigeria and technical brochures of manufacturers of the mooring lines used in the project, other literature and personal communication with industry personnel. The sizes of the components of the designed line. Then, the load acting on the line of the project were used as initial sizes and estimated load. Component cost data was acquired from the work of Klingan (2016) in Norwegian Krone and converted to the dollar by the rate of (1USD = 9.117NOK) as quoted by the Norwegian central bank, Norges bank (2019), while pre-installation cost was obtained from personal communication. Other input data are derived from the material of the recent project or are constraints imposed on the lines. In Table 1, cost per unit dry weight for the chain is symbolized as  $C_{N1,3}$ , for the bottom and top chain, respectively. Costs per unit dry weight for wire rope and polyester are both symbolized as  $C_{N2}$ . This is because the computation for the chain-wire-chain configuration was repeated, with some different input data, for the chain-polyester-chain configuration.



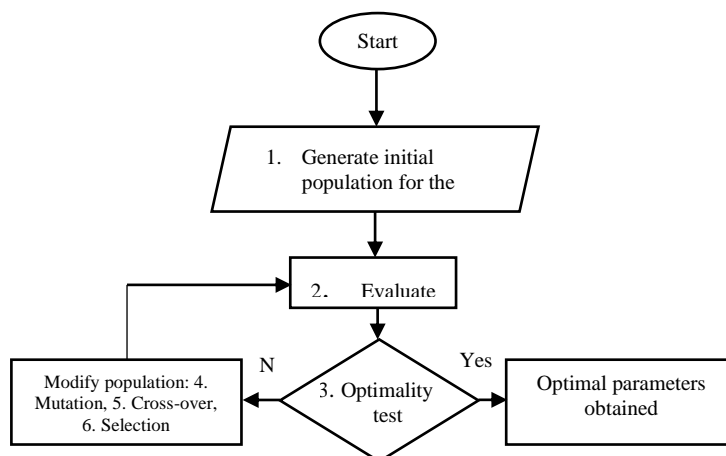


**Figure 2: Genetic algorithm procedure (Source: Cao and Wu, 1999; Haupt and Haupt, 2004)**

**Table 2 Input data**

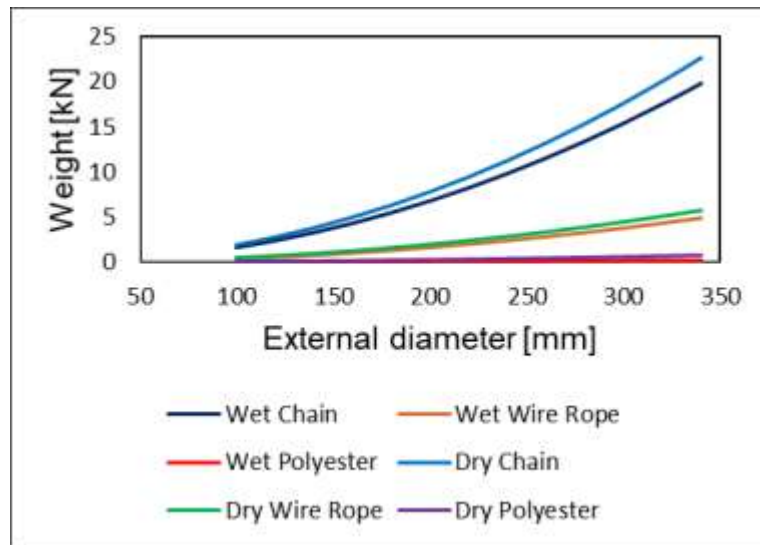
S/No	Quantity	Symbol	Unit	Value
1	Water depth	$h$	m	1473
2	The diameter of the top chain	$d_{c2}$	mm	157
3	The diameter of the bottom chain	$d_{c1}$	mm	147
4	The diameter of the wire rope	$d_w$	mm	140
5	The polyester diameter of equivalent wire rope strength	$d_p$	mm	265
6	Depth of top chain	$h_1$	m	100
7	External load	$W$	MN	44
8	The angle of the line to horizontal at TDP	$\theta$	deg	25
9	Cost of chain	$C_{N1,3}$	\$/N	0.275
10	Cost of wire rope	$C_{N2}$	\$/N	0.55
11	Cost of polyester	$C_{N2}$	\$/N	0.77
12	Day rate of a vessel for pre-installation	$C_{iv}$	\$/day	75944
13	Installation rate	$I_r$	Line/day	1

## RESULTS AND DISCUSSION

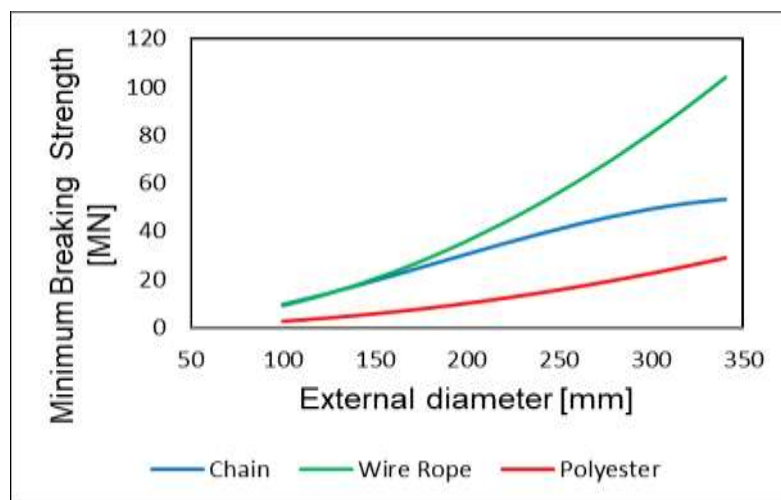
### Results

Table 2 shows some results of the computation which was done in EES. The result shown is for a design of maximum allowable tension on the mooring line, derived from equation (9). The first section of Table 2 shows the chain properties which are common to both the chain-wire-chain (C-W-C) configuration and the chain-polyester-chain (C-P-C) configuration. Figures 3 and 4 are graphs of the calculated properties of the chain, wire rope and polyester materials. The graphs are beneficial to understand the cost performance of the mooring line. The mooring profiles of the chain-wire-chain and chain-polyester-chain configurations are shown in Figure 5. The depths and horizontal distances of the components of the different configurations were computed

from the taut multi-component mooring equations, Equations (9) through (14), and plotted to obtain Figure 5. The load on a floating structure determines the size, the number of lines and the cost of the system, eventually. Cost of the system was plotted against varying loads. The number of lines required to overcome the load is also shown in the plot, Figure 6. The length of line and thus horizontal distance is partly dependent on the angle of the mooring line to the horizontal at touch down point. The relationship of the angle to the cost of a single chain-wire-chain line is plotted and shown in Figure 7.



**Figure 3 Weights of mooring materials**



**Figure 4 Minimum breaking strength of mooring materials**

**Table 3 Computation results**

S/No	Output	Unit	Value
1	Wet weight of top chain	N/m	4215
2	Wet weight of bottom chain	N/m	3695
3	MBL of top chain	MN	21.23
4	MBL of bottom chain	MN	19.09
Chain-Wire-Chain configuration			
5	Wet weight of wire rope	N	842.2
6	MBL of wire rope	MN	17.64
7	Length of top chain	m	150.7
8	Length of bottom chain	m	315.3
9	Length of wire rope	m	2077
10	Total length	m	2543
11	Tension	MN	8.467
12	Horizontal distance	m	2066
13	Number of lines	-	7.9
14	Cost per line	M\$	1.628
15	Total cost	M\$	13.46
Chain-Polyester-Chain configuration			
16	Wet weight of polyester	N	119.4
17	MBL of polyester	MN	17.56
18	Length of top chain	m	176.2
19	Length of bottom chain	m	317
20	Length of polyester	m	2302
21	Total length	m	2795
22	Tension	MN	8.427
23	Horizontal distance	m	2374
24	Number of lines	-	7.3
25	Cost per line	M\$	1.145
26	Total cost	M\$	8.908

**Effects of line size and pre-installation cost**

Effects of line size and pre-installation cost on the combined cost, the sum of manufacturing cost and pre-installation cost, are investigated. For the chain-wire-chain configuration, similar sizes of chain and wire are utilized in the design. Manufacturing cost and combined cost, as well as a number of lines, are plotted against line sizes and are shown in Figures 8 and 9, respectively.

For the chain-polyester-chain configuration, due to the more increased difference in minimum breaking strength of similar sizes of chain and polyester, sizes of similar minimum breaking strength were used in the investigation. The size combinations of

the chain and polyester, as well as the number of lines required to overcome the load, are shown in Table 3. Column charts, Figures 10 and 11, show the manufacturing cost and the combined cost of the several combinations of sizes of chain and polyester. Figures 8, 9, 10 and 11 were plotted from results of computation carried out with the load on the system as 44MN and the angle of the line to the horizontal at TDP as 25°.

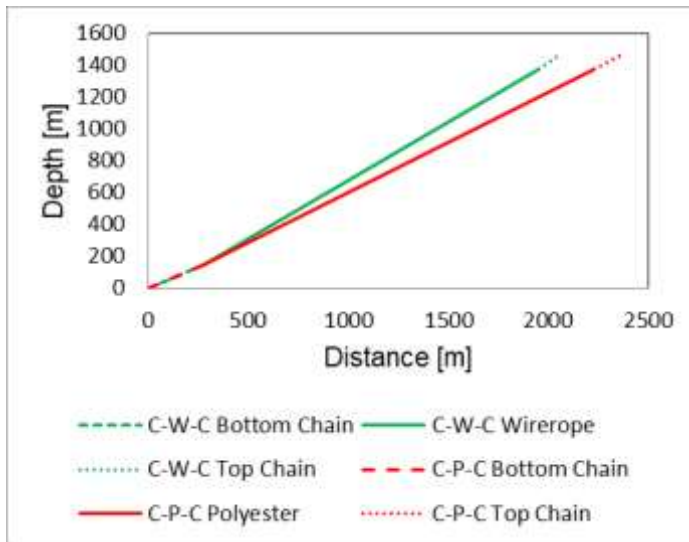


**Figure 5 Mooring line profiles of multi-component mooring**

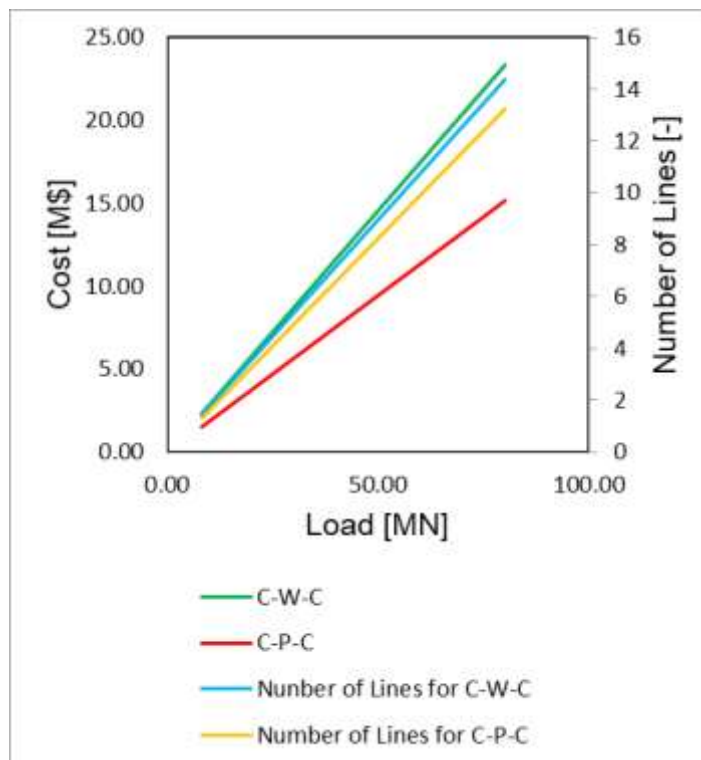


**Figure 6 Cost of lines at varying loads**

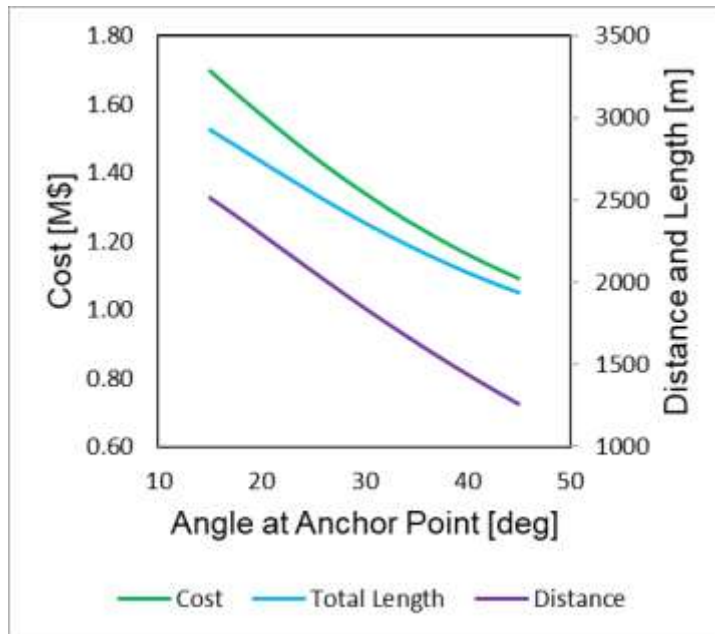


Figure 7 Cost of Chain-Wire-Chain line with respect to angle at the seafloor, the total length of line and horizontal distance

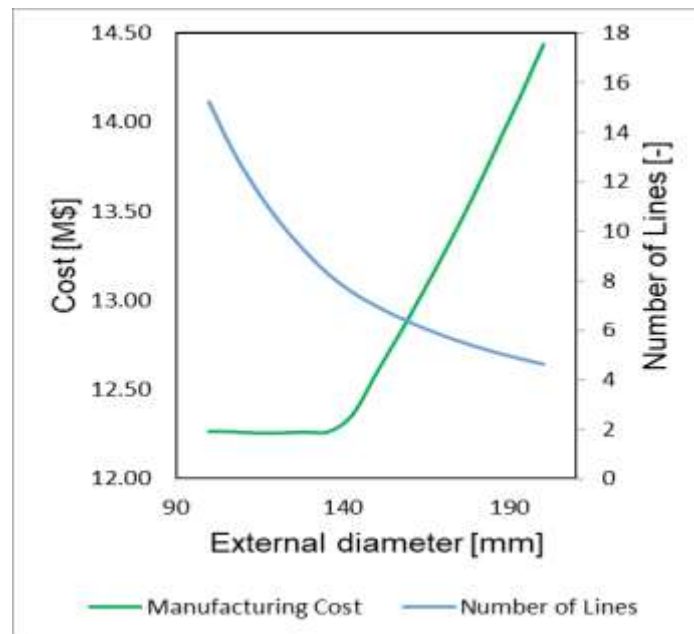
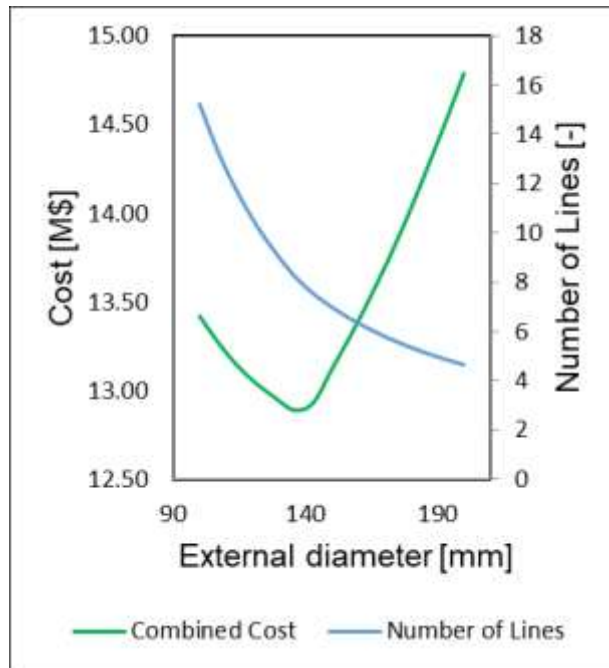
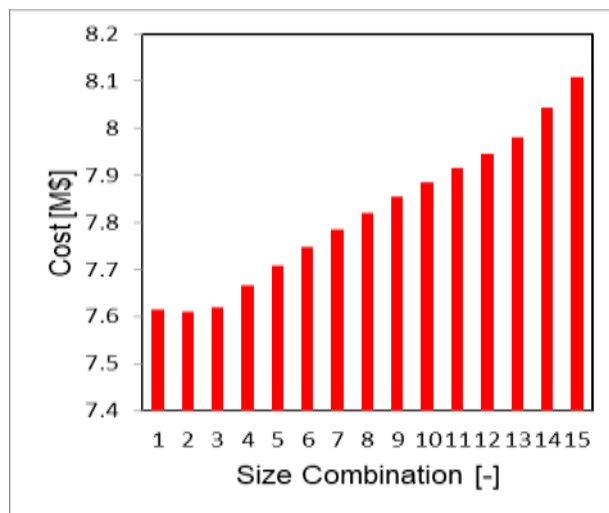


Figure 8 Manufacturing cost of Chain-Wire-Chain line with respect to line size and number of lines



**Figure 9** Combined cost of Chain-Wire-Chain line with respect to component sizes and number of lines



**Figure 10** Manufacturing cost of Chain-Polyester-Chain for various size combinations

**Table 4 Costs of several size combinations for Chain-Polyester-Chain line**

Size Combination	Diameter [mm]			Number of Lines [-]
	Polyester	Bottom Chain	Top Chain	
1	200	100	100	12.8
2	208.2	105.1	105.1	11.71
3	216.4	110.3	110.3	10.79
4	224.6	115.4	115.4	10.02
5	232.9	120.6	120.6	9.336
6	241.1	125.7	125.7	8.717
7	249.3	130.9	130.9	8.158
8	257.5	136	136	7.651
9	265.7	141.1	141.1	7.19
10	273.9	146.3	146.3	6.77
11	282.1	151.4	151.4	6.385
12	290.4	156.6	156.6	6.032
13	298.6	161.7	161.7	5.716
14	306.8	166.9	166.9	5.446
15	315	172	172	5.199

**Optimisation**

From the investigation of the effect of line size and pre-installation cost on the combined cost of a system, there is a need to find optimal sizes for a minimum cost of the system while meeting the minimum tension constraint on a line. The optimisation was done in EES with the genetic algorithm. The result of the optimisation is shown in Table 4. The optimisation was done at a load of 44MN and the angle at TDP of 25°.

**Table 5 Optimal sizes of lines for C-W-C and C-P-C configurations**

Parameter	Unit	Value
Chain-Wire-Chain		
Diameter of top chain	mm	135.00
Diameter of bottom chain	mm	135.00
Diameter of wire rope	mm	135.7
Number of lines	-	8.27
Combined Cost	M\$	12.90
Chain-Polyester-Chain		
Diameter of top chain	mm	135.90
Diameter of bottom chain	mm	135.90
Diameter of polyester	mm	259
Number of lines	-	7.56
Combined Cost	M\$	8.36

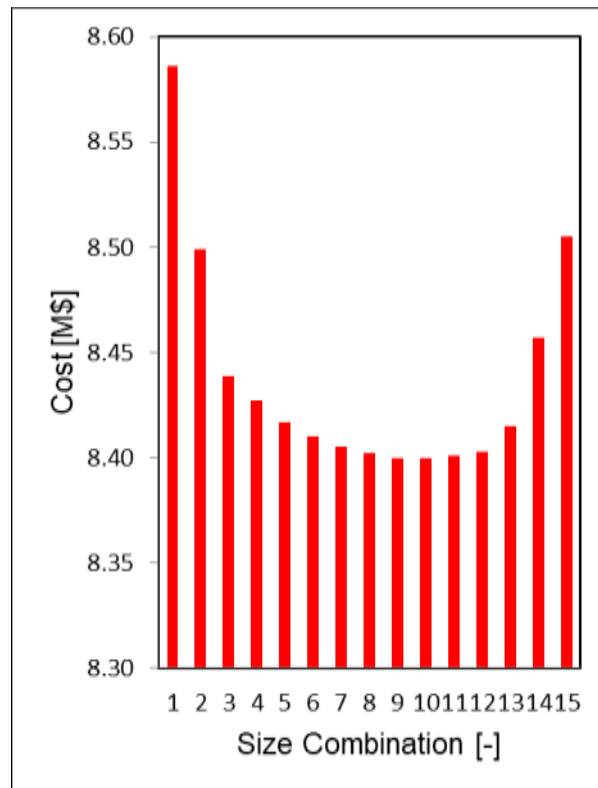


**Figure 11 Combined cost of Chain-Polyester-Chain for several size combinations**

## DISCUSSIONS

The analysis done has shown that the properties and cost of a mooring line largely depend on the size of the line. Polyester ropes are much lighter than wire ropes and chain but require bigger sizes to possess equivalent strength, as shown in figures 3 and 4. The properties of the materials determine the performance of the system to a great deal. Figures 3 and 4 are very useful in understanding the effect of the line size and pre-installation cost. The chain-polyester-chain configuration spans over a longer horizontal distance than the chain-wire-chain configuration as can be seen in Figure 5. This is due to the lighter weight of the polyester material. The additional length of the polyester compensates for the weight with the design tension of the minimum MBL of the components of the line From Table 2; the bottom chain has a minimum of MBL.

With the data specified in Table 1, Figure 6 provides estimates of the manufacturing costs and a number of lines required to sustain computed external loads acting on a floating structure in deep water. The angle of the mooring line at TDP determines the length of the line, horizontal distance and hence the anchor radius. This is project-specific, however. If a project requires equipment such as risers and umbilicals to be tied into a floating platform, the angle of the line at TDP will be lesser, which will increase the length of the line and consequently, its cost. Mobile Offshore Drilling Units (MODUs) will use larger angles than permanent floating structures, but their



lines have to be long enough to prevent vertical uplift force on the anchors. MODUs utilize drag embedment anchors which are more mobile, as opposed to driven piles and suction piles which are fixed. Drag embedment anchors are only designed to withstand horizontal loads.

The investigations on the effect of line size per cost show that an increase in the size of the line reduces the number of lines required for the application. However, the increasing cost of the size of the line balances the cost reduction from reducing the number of lines. The increase in the sizes of the mooring line produces an increased cost. This condition eliminates gains from a cost reduction of reducing the number of lines. It causes a net increase in the manufacturing cost of the lines of the system despite a further reduction in line number, as shown in Figures 8 and 10 for C-W-C and C-P-C configurations, respectively.

When pre-installation costs are incorporated into the analysis, Figures 9 and 11 show that there is an initial high combined cost of manufacturing and pre-installation, due to the higher number of lines. Increasing the diameters of the lines reduces combined cost until a minimum cost is achieved. Further increase in diameter causes increasing costs depending on line size to outweigh cost reductions from reducing line number, resulting in a net cost increase. Figures 9 and 11 rely strongly on the pre-installation cost. An increase or decrease will cause the minimum to move right or left.

Minimum cost is obtained by finding optimal sizes of the lines for the C-W-C and C-P-C configurations with the genetic algorithm in EES. From Table 4, it can be seen that there is a 35% reduction in cost when the C-P-C configuration is used over the C-W-C configuration.

## CONCLUSIONS AND RECOMMENDATIONS

### Conclusions

There is a great need to find optimal station keeping cost solutions as human activities move further offshore into deeper waters, especially for permanently moored structures. Relevant literature in the area of mooring design was reviewed, and it was observed that adequate knowledge is not known when installation costs are incorporated into the cost analysis. This work thus attempts to bridge that gap in knowledge. A techno-economic model based on taut multi-component quasi-static equations and simple cost relations was developed for this work. The work compares two mooring line component configuration; chain-wire-chain (C-W-C) and chain-polyester-chain (C-P-C), and optimisation was done using the genetic algorithm incorporated into EES. It was found that:

1. A chain-polyester-chain configuration will span a longer horizontal distance than a chain-wire-chain configuration at the same load.
2. The length of line and a horizontal distance of the lines inversely depend on the angle at TDP.
3. The number of lines increases with increasing load, resulting in increased costs.
4. Cost reduction from increasing component sizes has a limit beyond which costs are increased astronomically.

5. The optimal combined cost is as a result of a trade-off between component sizes and the number of lines. This depending on the cost of pre-installation

From Table 4, it can be concluded that the use of chain-polyester-chain has a 35% cost reduction on the use of a chain-wire-chain configuration. In reality, however, the installation rate and thus, installation costs of polyester and wire rope may not be similar. To avoid excessive pretension adjustments due to bedding-in effect and permanent elongation of polyester ropes in service. It is recommended that a pre-stretching of the polyester rope by the use of an additional vessel is done (DeAndrade and Duggal, 2010). This will increase the installation rate and the number of days of operation, thus increasing the cost of using the installation vessel. Furthermore, the utilization of an additional vessel for the pre-stretching operation will result in increased costs.

### **Recommendations**

Assumptions were made to simplify this work. In reality, however, additional work has to be done for a complete analysis. Also, there are additional costs that have to be considered. Thus, for the advancement of this study, it is recommended that:

1. A dynamic analysis, considering added mass, damping and fluid acceleration, should be done by using an appropriate mathematical method to solve equation (15). The finite element method is the most popular method for solving the equation. A finite-difference could be done and compared with the finite element method.
2. Appropriate anchor and on-vessel equipment selection should be made.
3. Lifting and transportation cost data should be obtained and incorporated into the cost analysis. Larger component sizes will increase lifting and transport costs and have to be considered.
4. Inspection, maintenance, repair and decommissioning costs should also be incorporated. Since polyester is a relatively new technology, test inserts are included in the line and occasionally retrieved for inspection (Ma et al., 2019). This will result in increased life cycle cost for the chain-polyester-chain system.
5. Performance of fatigue analysis is to establish the reliability and fatigue life of the system. The Palmgren-Miner's rule of S-N or T-N curves or a fracture mechanics approach can be used to estimate the fatigue damage (Xue et al., 2018).

Results of this work have shown that installation costs must be factored into the decision process of selecting an optimal cost solution in the design of mooring systems. Depending on the installation cost, an optimal cost solution is a trade-off between line size and the number of lines.

Also, from the properties of the components for deepwater multi-component mooring lines, it is important to select components with close MBS's. The load-carrying capacity of a line is limited by the minimum MBS of the components of that line, which determines maximum tension on the line. Large differences in component strengths will result in increased costs wherein the extra strength from the stronger component will be wasted, resulting in unnecessary costs. From the optimisation results, for the chain-wire-chain configuration, the strength of a wire rope of size

135.7mm is 16.57MN and strength of chain of R4 grade of size 135mm is 16.58kN. Similarly, for the chain-polyester-chain configuration, the strength of polyester of size 259m is 16.77kN and strength of chain of R4 grade of size 135.9mm is 16.76kN. It is important to minimize chain diameter due to the higher weight of the chain and the cost associated with its weight.

## References

- Banfield, S. and Casey, N. (1997) Evaluation of fibre rope properties for offshore mooring, *Ocean Engineering*, 25(10), pp. 861-879.
- Cao, Y. J. and Wu, Q. H. (1999) Teaching Genetic Algorithm Using Matlab, *International Journal of Electrical Engineering and Education*, 36, pp. 139-153, DOI: 10.7227/IJEEE.36.2.4
- Chakrabarti S. (2005) *Handbook of offshore engineering*, Elsevier limited, London.
- Charbonneau, P. (1995) *Genetic Algorithms in Astronomy and Astrophysics*, The Astrophysical Journal Supplement Series, The American Astronomical Society, U.S.A, 101 pp 309-334,
- Charbonneau, P. (2002) *An Introduction To Genetic Algorithms For Numerical Optimisation*, NCAR Technical Note, National center For Atmospheric Research, Colorado
- Figueiredo, P. A. and Brojo F. M. (2017) Parametric study of multi-component mooring lines at catenary form in terms of anchoring cost, 4th International Conference on Energy and Environmental Research, Porto, Portugal, 136, pp 456-462, DOI: 10.1016/j.egypro.2017.10.303
- F-Chart Software, Genetic Method, Available at: [http://fchartsoftware.com/ees/eeshelp/genetic\\_method.htm](http://fchartsoftware.com/ees/eeshelp/genetic_method.htm) [Accessed November 10, 2019].
- Gongcheng Zhang, Hongjun Qu, Guojun Chen, Chong Zhao, Fenglian Zhang, Haizhang Yang, Zhao Zhao and Ming Ma (2019) Giant discoveries of oil and gas fields in global deepwater in the past 40years and the prospect of exploration, *Journal of Natural Gas Geoscience*, 4, pp. 1-28, DOI: 10.1016/j.jnggs.2019.03.002.
- Haupt, R. L. and Haupt, S. E. (2004). *Practical Genetic Algorithm*. New York: John Wiley & Sons, Ltd.
- Henry S. Pettingill and Paul Weimer (2002) *World-Wide Deepwater Exploration and Production: Past, Present and Future*, Offshore Technology Conference, Houston, Texas, U.S.A.
- High Altitude Observatory, PIKAIA, National Center for Atmospheric Research, Colorado, Available at <http://www.hao.ucar.edu/modeling/pikaia.php> [Accessed November 10, 2019]
- Jonas Bjerg Thomsen, Francesco Ferri, Jens Peter Kofoed and Kevin Black (2018) Cost Optimisation of Mooring Solutions for Large Floating Wave Energy Converters, *Energies*, 11, 159; DOI: 10.3390/en11010159
- Jun Sik Han, Yun Ho Kim, Young-Jun Son and Hang S. Choi (2010) A comparative study on the fatigue life of mooring systems with different composition, 9th International Conference on Hydrodynamics, October 11-15, Shanghai, China, 22(5), pp. 452-456, DOI: 10.1016/S1001-6058(09)60235-3

- Kai-Tung Ma, Yong Luo, Thomas Kwan and Yongyan Wu(2019) Mooring System Engineering for Offshore Structures, Elsevier Incorporated, DOI: 10.1016/B978-0-12-818551-3.00001-6
- Klingan, K. E. (2016) Automated Optimisation and Design of Mooring Systems for Deep Water, Norwegian University of Science and Technology, Available at <http://hdl.handle.net/11250/2409562> [Accessed September 02, 2019].
- Kyoung-Hyun Lee, Hyung-Suk Han and Sungho Park (2015) Failure analysis of naval vessel's mooring system and suggestion of reducing mooring line tension under ocean wave excitation, *Engineering Failure Analysis*, 57, pp. 296-309, DOI: 10.1016/j.engfailanal.2015.08.005
- MathWorks, How the Genetic Algorithm Works, MathWorks, Available at <https://www.mathworks.com/help/gads/how-the-genetic-algorithm-works.html> [Accessed November 05, 2019].
- Mavrakos, S. A.; Papazoglou, V. J.; Triantafyllou, M. S. and Hatjigeorgiou J. (1994) Deepwater mooring dynamics, *Marine Structures*, 9, pp 181-209.
- Mir Emad Mousavi and Paolo Gardoni (2014) A simplified method for reliability- and integrity-based design of engineering systems and its application to offshore mooring systems, *Marine Structures*, 36, pp. 88-104, DOI: 10.1016/j.marstruc.2014.02.001
- Mitchell Melanie (1999) *An Introduction to Genetic Algorithms*, A Bradford Book The MIT Press, Massachusetts, pp 2, ISBN 0-262-13316-4(HB), 0-262-63185-7 (PB)
- Mohammad Saidee Hasan (2016) A Simplified Method for Analyzing the Fatigue Life of a FPSO Mooring System, 10th International Conference on Marine Technology, MARTEC, 194, pp. 502-508, DOI: 10.1016/j.proeng.2017.08.177
- Nielsen, F. G. and Bindingbo, A. U. (2000) Extreme loads in taut mooring lines and mooring line induced damping: an asymptotic approach, *Applied Ocean Research*, 22, pp. 103-118.
- Norges Bank, Exchange rates, Norges bank, Available at [https://www.norges-bank.no/en/topics/statistics/exchange\\_rates/?tab=currency&id=](https://www.norges-bank.no/en/topics/statistics/exchange_rates/?tab=currency&id=) [Accessed November 4, 2019]
- Omar DeAndrade and Arun Duggal (2010) Analysis, Design and Installation of Polyester Rope Mooring Systems in Deep Water, Offshore Technology Conference, Houston, Texas, USA
- Sam Ryu, Arun S. Duggal, Caspar N. Heyl and Zong Woo Geem (2016) Cost-Optimized FPSO Mooring Design Via Harmony Search, *Journal of Offshore Mechanics and Arctic Engineering*, 138, DOI: 10.1115/1.4034374
- Shaoji Fang, Mogens Blanke and Bernt J. Leira (2015) Mooring system diagnosis and structural reliability control for position moored vessels, *Control Engineering Practice*, 36, pp. 12-26, DOI: 10.1016/j.conengprac.2014.11.009
- Sheng Xua, Chun-yan Ji and Guedes Soares, C. (2018) Experimental and numerical investigation a semi-submersible moored by hybrid mooring systems, *Ocean Engineering*, 163, pp. 641-678, DOI: 10.1016/j.oceaneng.2018.05.006
- Skop, R. A. (1988) Mooring Systems: A State-of-the-Art Review, *Journal of Offshore Mechanics and Arctic Engineering*, 110/365.

Tetlow, J. and Leece, M. (1982) Hutton TLP Mooring System, 14<sup>th</sup> Annual Offshore Technology Conference, Houston, Texas.

Vahid Hassani, Antonio M. Pascoal and Asgeir J. Sørensen (2018) Detection of mooring line failures using Dynamic Hypothesis Testing, Ocean Engineering xxx, pp. 1-8, DOI: 10.1016/j.oceaneng.2018.01.021

Xutian Xue, Nian-Zhong Chen, Yongyan Wu, Yeping Xiong and Yunhua Guo (2018) Mooring system fatigue analysis for a semi-submersible, Ocean Engineering, 156, pp 550-563, DOI: 10.1016/j.oceaneng.2018.03.022